



## Digital phantoms for the evaluation of a software used for an automatic analysis of the Winston-Lutz test in image guided radiation therapy

Tarraf Torfeh, Stéphane Beaumont, David Bonnet, Yves Barbotteau, Jean-Pierre Guédon, Nicolas Normand, Eloïse Denis, Pascal Fenoglietto, Norbert Ailleres

### ► To cite this version:

Tarraf Torfeh, Stéphane Beaumont, David Bonnet, Yves Barbotteau, Jean-Pierre Guédon, et al.. Digital phantoms for the evaluation of a software used for an automatic analysis of the Winston-Lutz test in image guided radiation therapy. *Medical Imaging 2008: Physics of Medical Imaging*, Feb 2008, San Diego, CA, USA, United States. 6913 (69133F), pp.69133F-69133F-11, 2008, <10.1117/12.768668>. <hal-00326648>

**HAL Id: hal-00326648**

**<https://hal.archives-ouvertes.fr/hal-00326648>**

Submitted on 4 Oct 2008

**HAL** is a multi-disciplinary open access archive for the deposit and dissemination of scientific research documents, whether they are published or not. The documents may come from teaching and research institutions in France or abroad, or from public or private research centers.

L'archive ouverte pluridisciplinaire **HAL**, est destinée au dépôt et à la diffusion de documents scientifiques de niveau recherche, publiés ou non, émanant des établissements d'enseignement et de recherche français ou étrangers, des laboratoires publics ou privés.



# Digital phantoms for the evaluation of a software used for an automatic analysis of the Winston-Lutz test in image guided radiation therapy

Tarraf Torfeh<sup>a, b</sup>, Stéphane Beaumont<sup>b</sup>, David Bonnet<sup>b</sup>, Yves Barbotteau<sup>c</sup>, JeanPierre Guédon<sup>a</sup>,  
Nicolas Normand<sup>a</sup>, Eloïse Denis<sup>a, b</sup>, Pascal Fenoglietto<sup>c</sup> and Norbert Ailleres<sup>c</sup>.

<sup>a</sup> IRCCyN/IVC – UMR CNRS 6597, Image & Video Communication, École polytechnique de  
l'Université de Nantes, La Chantrerie, BP 50609, 44306 Nantes Cedex 3 – France

<sup>b</sup> QualiFormeD SARL, Centre Hospitalier Départemental, 85925 La Roche Sur Yon, France

<sup>c</sup> Centre Régional de Lutte Contre le Cancer, Val d'Aurelle, 34298 Montpellier, France

## ABSTRACT

Accurate isocentre positioning of the treatment machine is essential for the radiation therapy process, especially in stereotactic radio surgery and in image guided radiation therapy.

We present in this paper a new method to evaluate a software which is used to perform an automatic analysis of the Winston-Lutz<sup>1, 2</sup> test used in order to determine position and size of the isocentre. The method consists of developing digital phantoms that simulate mechanical distortions of the treatment machine as well as misalignments of the positioning laser targeting the isocentre. These Digital Test Objects (DTOs) offer a detailed and profound evaluation of the software and allow determining necessary adjustments which lead to high precision and therefore contributes to a better treatment targeting.

**Keywords:** PHT, SIM, METR, CT.

## 1. INTRODUCTION

The main objective of the Winston-Lutz<sup>1</sup> (WL) test is to control the position and the size of the isocentre of a medical linear accelerator (LINAC) i.e. the intersection of the gantry, the collimator and the couch axis. This control allows accurate alignment of the room laser system which is essential for the success of the radiotherapy and avoids systematic errors of irradiation localization which have serious consequences on the treatment process. An example of these sequences would be the excessive irradiation of the healthy tissues surrounding the tumor while the tumor itself is under irradiated. Furthermore, the emerging image guided radiation therapy gives this test a new actuality. Here the size of the isocentre affects directly the image quality of the cone beam CT mode<sup>3, 4</sup>, and the position of the isocentre determines the precision of the patient repositioning. The test proposed by Winston & Lutz is also able to quantifying the sensor movement during the rotation process<sup>2, 5</sup>.

The use of digital phantoms in order to control the quality of RT medical images treatment platform has being previously proposed by Denis et al<sup>6</sup>, and was used in order to test Virtual Simulation Softwares<sup>7</sup>. This technique has a lot of advantages, especially the perfect knowledge of the software data input. But also the possibility of an automation of the quality control procedure by comparison of the processing of this input data with an output digital phantom designed to be a reference for this processing can be mentioned. This paper presents a complete application of this recent concept and therefore a method of developing digital phantoms included calibrated misalignments of the isocenter that allows evaluating the performances of software tools that are dedicated for an automatic quality control of the Winston & Lutz test (WL test).

These evaluations allow, in one hand, studying the influence of all adjustment parameters of the software which leads to the determination of an optimal set of this parameters, and in the other hand, using these optimal values we can determine the precision of the software and the method proposed by Winston & Lutz.<sup>1</sup>

---

<sup>a</sup> tarraf.torfeh@univ-nantes.fr, <sup>b</sup> stephane.beaumont@qualiformed.com, Telephone: +33 (0)8 77 00 91 29

## 2. MATERIALS AND METHODS

### 2.1 The real test

The Winston-Lutz test consists of aligning a 5 mm diameter tungsten ball on the room lasers (i.e. the supposed location of machine isocentre) and to acquire different two-dimensional (2D) projection images on it for different gantry, table and collimator rotation angles. The tungsten ball is held by an acrylic (PMMA) tube which is fixed on the treatment couch. In IGRT technique, the 2D images are produced by the RX treatment source (2D-MV mode) and a flat panel mounted in opposition and by an additional RX tube and a second flat panel (2D-kV mode). In IGRT application, the Winston-Lutz test controls the position and the size of the kV and MV isocenters but also the movement of the 2 flat panels during the rotation of the gantry. Though, for the movement of the flat panel the reference position in the images is the flat panel center. But for the isocenter location and size the reference point in the images is the middle of a 5 x 5 cm<sup>2</sup> beam. Three units are involved in the control, collimator, gantry and couch; therefore the control process consists of rotating one unit while keeping the two other units stationary. Two-dimensional images corresponding to different angles of rotation are then acquired. Theoretically and if the collimator and table axis were exactly aligned and the physical test object is placed correctly, we obtain images where the pixel representing the centre of the tungsten ball is always placed in the centre of the beam image representing the irradiation field. Figure 1 shows the treatment machine on the left, Winston and Lutz test homemade phantom and on the right, an example of 2D image of the phantom.

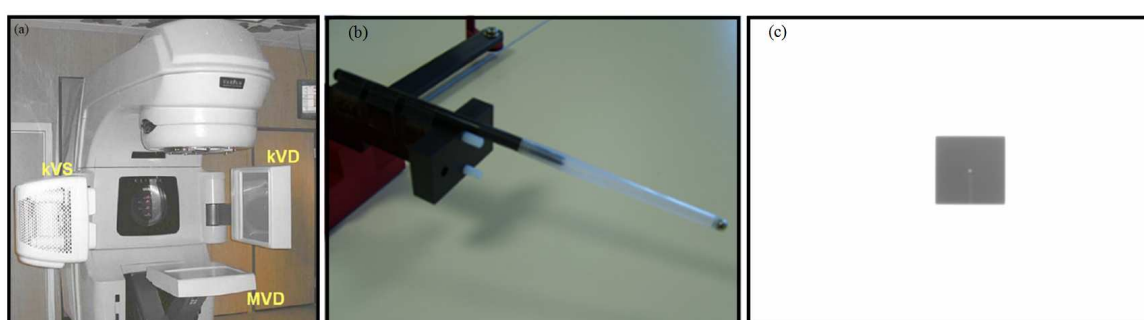


Fig. 1. (a) Treatment machine with an On-Board Imager (OBI) consisting of two arms; one holding an X-ray source and one holding a flat panel sensor. A megavoltage detector (MVD) is also showed. (b) The phantom proposed by Winston and Lutz consisting of a 5mm tungsten ball held in a PMMA mounting. (c) A two-dimensional image of this phantom, where the shadow of the tungsten ball and the beam can be visualized.

### 2.2 QFD-WL software module

The QFD-WL<sup>8,9</sup> module is embedded in a platform QFD-IQC commercialized for an automatic analysis of the image produced for the image quality control in medical imaging and radiation therapy.

The automatic software analysis is organized in the QFD-IQC-WL module in 8 steps:

1. Decoding of the DICOM RT images directly transferred from the treatment machine by the network
2. Image pre-processing: limiting - scaling with nearest neighbors, bilinear or bi-cubic interpolation (Figure 2)
3. Determination of the radiation field center location in all images: threshold method (Figure 3)
4. Determination of the tungsten ball location in all images: convolution method (Figure 4)
5. Determination of the gantry rotation axis: back-projection method (Figure 5)
6. Determination of the table rotation axis: minimizing the parameter  $p$  (equation 1). Radiation field position considered as reference point (Figure 6)
7. Determination of the collimator rotation axis: minimizing the parameter  $p$  (equation 1). Tungsten ball position considered as reference point (Figure 6)
8. Calculation of the isocentre location: minimization of all units' isocentres.

In the four initial steps (steps 2, 3, 4 and 5) the user can choose different adjustments of the image processing (interpolation method, threshold value, size of the convolution kernel...). One goal of DTOs described in this paper is to study easily the influence of these different parameters on the software precision.

### 2.2.1 Image pre-processing

This process includes two steps: creating a new image with a size that represents a percentage value of the original image size and scaling the resulting image with a scale factor chosen by the user.

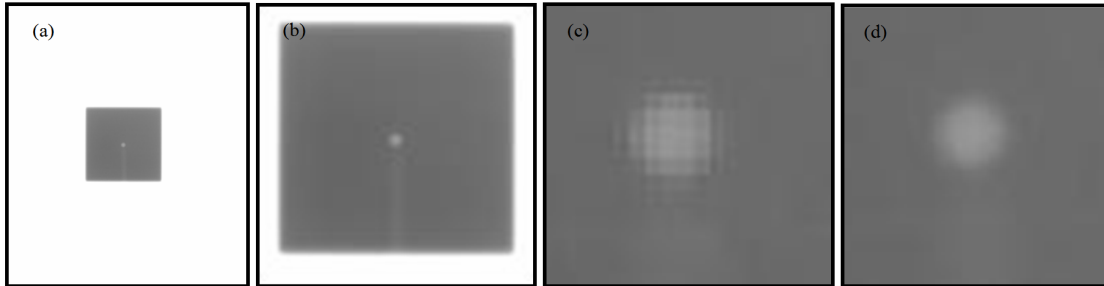


Fig. 2. (a) Original image. (b) Limited image and its 4 times scaling with, (c) nearest neighbor interpolation and (d) bi-cubic interpolation.

### 2.2.2 The radiation field center location

The radiation field center location is calculated by segmenting the image using a special threshold derived from its pixels intensity.

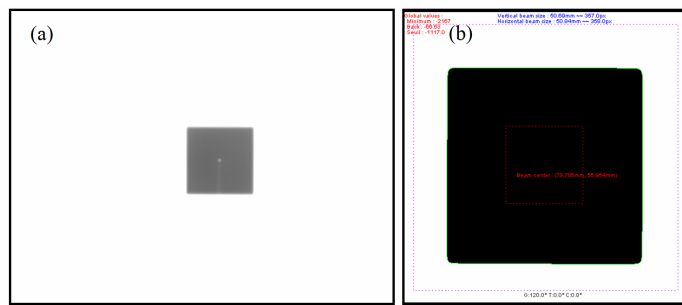


Fig. 3. Determination of the radiation field. (a) Original image. (b) Bi-level image representing the segmentation of the radiation field with a threshold equal to -1117.

### 2.2.3 The tungsten ball center location

A convolution of a Gaussian kernel with the radiation field image is used in order to find the centre of the tungsten ball image.

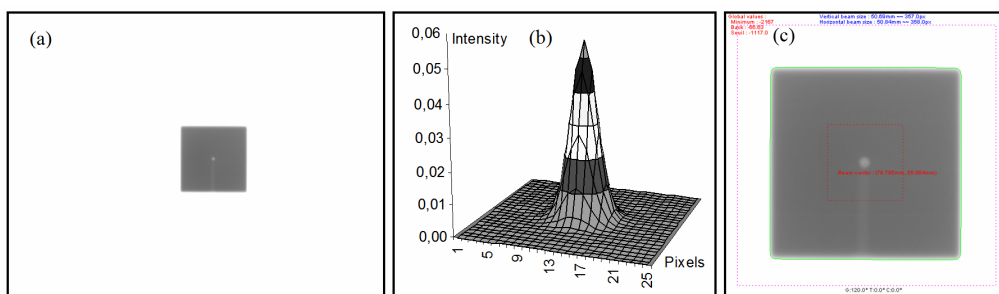


Fig. 4. Determination of the tungsten ball location. (a) Original image. (b) The two-dimensional Gaussian kernel used in the convolution method. (c) Image representing the position of the tungsten ball.

### 2.2.4 Gantry rotation axis

The positions of the tungsten ball with respect to the beam center are calculated; the 3D scene is then reconstructed by doing a back projection of these positions; a straight line perpendicular to the sensor plane that passes through the tungsten ball position is constructed (Figure 5).

Points of intersections between these lines are calculated and the position of the gantry rotation axis is then the gravity centre of these points.

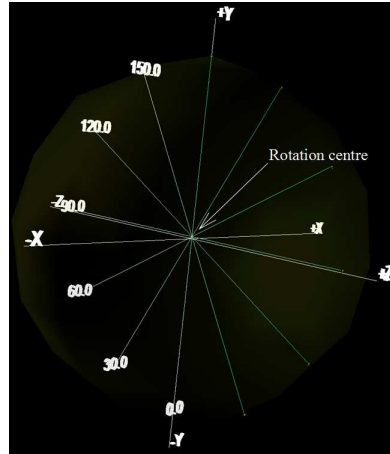


Fig. 5. Three-dimensional scene reconstruction. Images used are acquired with the collimator and the table at 0° position, while moving the gantry angle. Six angles are used in this example (0, 30, 60, 90, 120, 130 and 150°), and the gantry rotation centre is displaced of 6mm with respect to the Y axis.

### 2.2.5 Table rotation axis

In this process, images are acquired with the collimator and the gantry at 0° position.

The position of the radiation field centre being stationary is used as reference point while the tungsten ball centre positions describe a semicircle around this point (Figure 6).

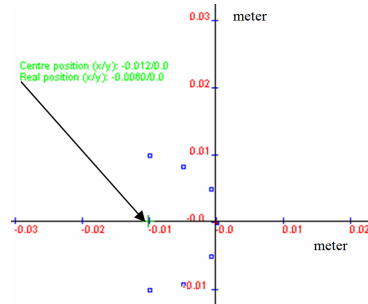


Fig. 6. Table/collimators rotation analysis. Six angles are used in this example (90, 120, 150, 180, 210, 240 and 270°), a displacement of 6 mm of the table/collimators rotation axis with respect to the X axis is introduced. The stationary point is represented with “□”, while “○” represent points describing a semicircle. The result found is 12 mm. This value was found on sensor level; knowing that the source sensor distance is 2 meters and the table sensor distance is equal to 1 meter, the real deviation value on (table level) is equal to 6mm.

In order to find the table rotation axis centre, the mean square error parameter p (equation 1) is minimized:

$$p(x, y) = \sum_i (d_i(x, y) - \bar{d})^2 \quad (1)$$

where (x, y) represents the coordinates of the circle centre,  $d_i$  is the distance from the centre of rotation to the shadow centre image, and  $\bar{d}$  indicates the mean value of all  $d_i$ .

### 2.2.6 Collimator rotation axis

The process here is similar to the table rotation axis analysis, with the difference that the reference point here is the tungsten ball instead of the radiation field centre.

### 2.2.7 Mechanical isocentre

The calculated isocentre of the gantry, table and collimator are projected on the plane formed by the lateral and longitudinal axis. These projections represent 3 points on this plane.

The position of the mechanical isocentre is on the line formed by the gantry rotation axis projection and parallel to longitudinal axis. This position is calculated by finding the point on this line has a minimum distance to the collimator/table projection points.

## 2.3 Digital Test Object (DTO)

In order to facilitate the quality control development process of the software algorithms and to test their limits, DTOs (Digital Test Objects) were generated. These DTOs represent a simulation of the images issued from the physical test object used for the test proposed by Winston and Lutz.

Many factors are involved in the production and formation of the images issued from a portal vision system: physical, geometrical...but since this study relay mainly on the position and the size of the patterns within the simulated images, only geometrical aspect are taken into consideration and substitutes physical aspects within the generated DTOs.

Several parameters representing the acquisition geometry, material and image properties, are used in order to generate DTOs. These parameters as well as other options are defined by the user through a graphical user interface developed for this purpose (Figure 7).

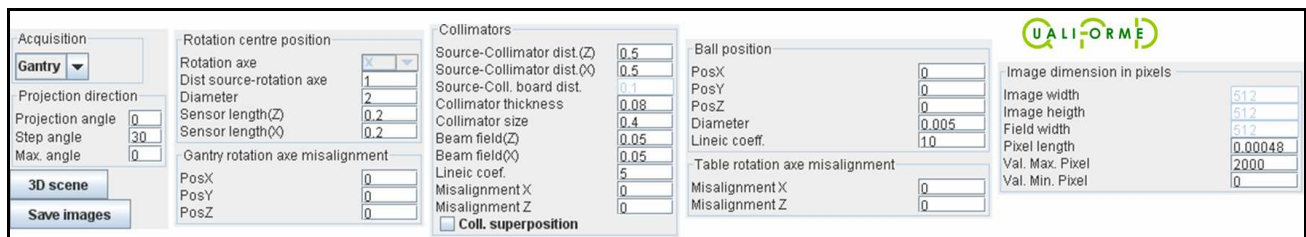


Fig. 7. Graphical user interface for the parameters of the Winston and Lutz DTOs. Acquisition geometry parameters: gantry rotation axis, source – rotation axis distance, acquisition diameter, source – collimator distance, ball position (x, y z), beam size, starting acquisition angle and step angle. Materials properties: sensor length, collimator thickness, collimator absorption coefficient, ball absorption coefficient.

### 2.3.1 Three-dimensional scene construction

Our objective is to create two-dimensional images, where each image represents the projection of the three-dimensional scene into the sensor, with respect to certain projection angle. Each pixel within images have an intensity proportional to the size of intersection between the materials in the three-dimensional scene (collimators and ball), and the ray formed from this pixel and the source point (source ray).

In order to do so, a three-dimensional scene is being constructed from all the parameters entered by the user (Figure 8).

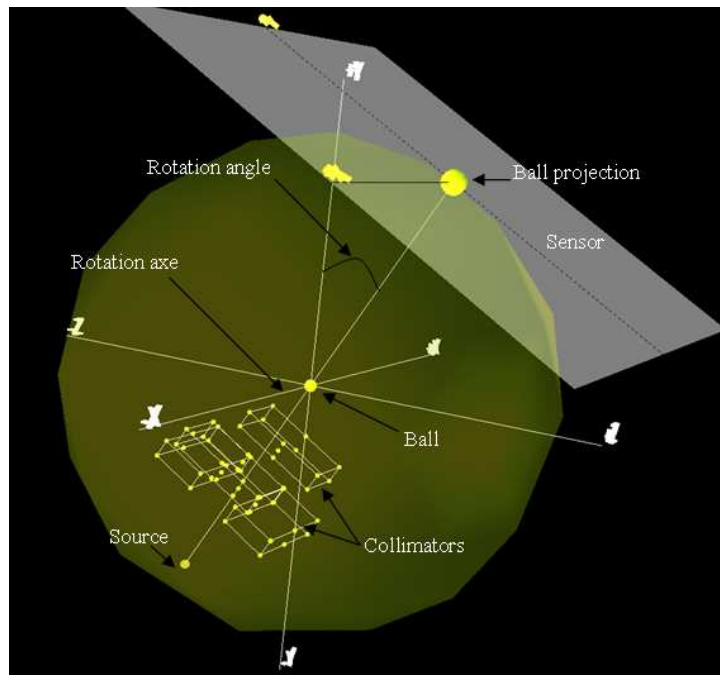


Fig. 8. Three dimensional reconstructed scene of the image acquisition process.

The first step of this process consists of finding the positions of the points representing respectively the source and the sensor centre. Knowing the rotation centre position, the projection angle and the rotation diameter, a line denoted (projection line) that passes through the rotation point and parallel to the angle of projection is constructed, so the position of the sensor centre is calculated from the intersection between the projection line and a sphere centered on the rotation centre with a diameter equals to the rotation diameter. Knowing the sensor centre position and the projection angle, the plane coefficient that passes through the sensor centre and perpendicular to the projection angle can be determined.

Using the same method, the position of the point representing the source centre is determined by changing the radius of the sphere used to calculate the intersection. The new sphere radius is equal to the source – rotation axis distance. Figure 9 shows the positions of the sensor and source points where, “X” is the rotation axis, the angle of projection is 30 degrees, the source-rotation axis distance is equal to 1 meter and the rotation diameter is equal to 2 meter.

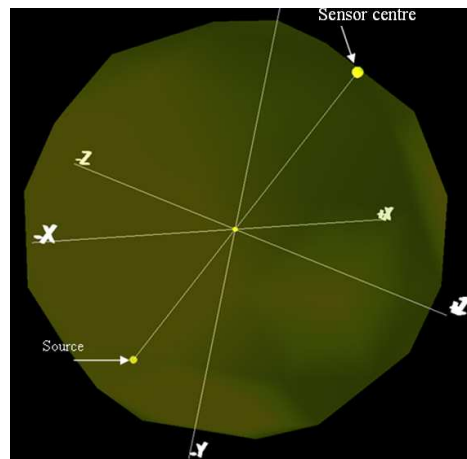


Fig. 9. Positions of the points representing the source and the sensor centre, the projection line with an angle of 30°.



Four collimator leaves are also created as shown in Figure 10 (a). A collimator leaf is represented with three planes as shown in Figure 10 (b). These planes will be used in order to find the size of the segment of the intersection between the collimator and the rays.

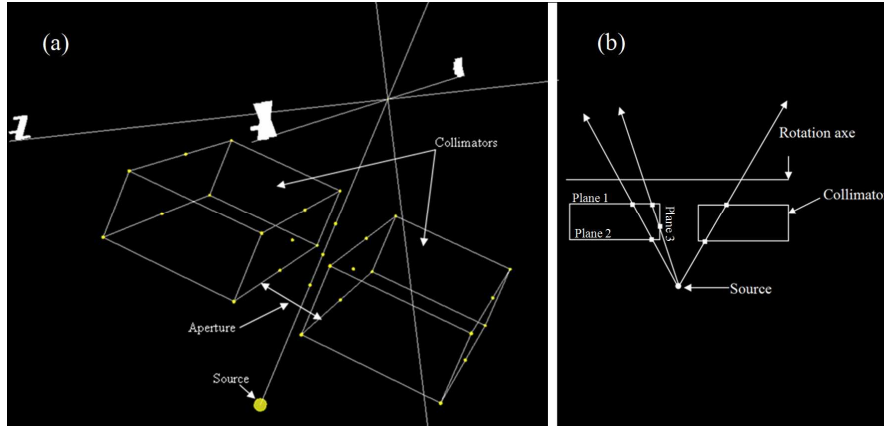


Fig. 10. (a) Two simulated collimator leaves with an aperture of 50mm, a thickness of 80mm and a source collimator distance of 500mm. (b) Planes used to find the segment of intersection between the source ray and collimators.

Knowing the collimator aperture and thickness, the segment of intersection between the source ray and the collimators can be calculated.

### 2.3.2 Two-dimensional image

A two-dimensional integer array of  $\left(\frac{\text{sensor\_length}}{\text{pixel\_length}}\right)^2$  size is created. This array represents the image issued from the flat panel sensor depicted in Figure 11. For each point in the 2D image, its 3D coordinate is calculated according to the projection angle. Three-dimensional coordinates of points within an image representing an angle of projection between 0 and 90° are equal to:

$$x_{3D} = x_{\text{sensor}} + \left(\frac{\text{width}}{2} - x_{2D}\right) \times \text{pixel\_length}$$

$$y_{3D} = y_{\text{sensor}} + \left(y_{2D} - \frac{\text{height}}{2}\right) \times \sin(\alpha) \times \text{pixel\_length}$$

$$z_{3D} = z_{\text{sensor}} + \left(y_{2D} - \frac{\text{height}}{2}\right) \times \cos(\alpha) \times \text{pixel\_length}$$

Where  $(x_{3D}, y_{3D}, z_{3D})$ ,  $(x_{\text{sensor}}, y_{\text{sensor}}, z_{\text{sensor}})$  are the three-dimensional coordinates respectively of the point and the sensor centre, *height* and *width* are the height and width of the two-dimensional image, and  $\alpha$  is the projection angle.

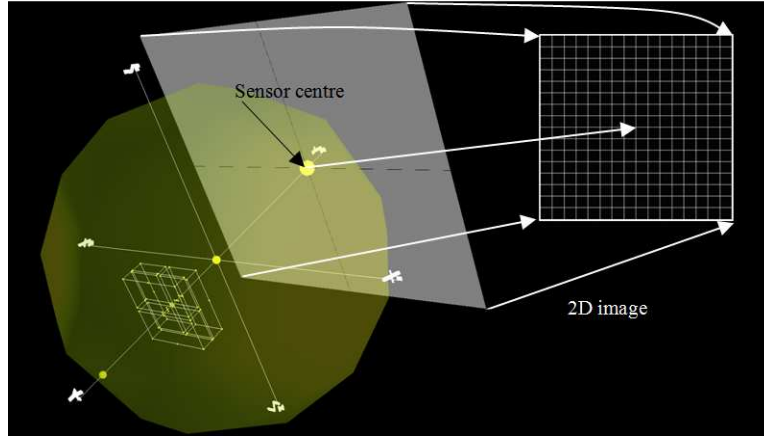


Fig. 11. Process of constructing a two-dimensional image from a three dimensional scene.

The value of the intensity of each pixel is based on the segment of intersection between the source ray and the materials in the three dimensional scene according to the formulae:

$$I_{Final} = I_0 \times \left( \frac{d_0}{dSC} \right)^2 \times e^{-\mu \times d}$$

where  $I_{Final}$  is the transmitted intensity (pixel intensity),  $I_0$  is the incident intensity,  $d_0$  is the incident distance ,  $dSC$  is the pixel source distance,  $\mu$  is the lineic absorption coefficient and  $d$  is the intersection thickness

Three types of DTO are simulated according to the acquisition type (gantry, collimator and table).

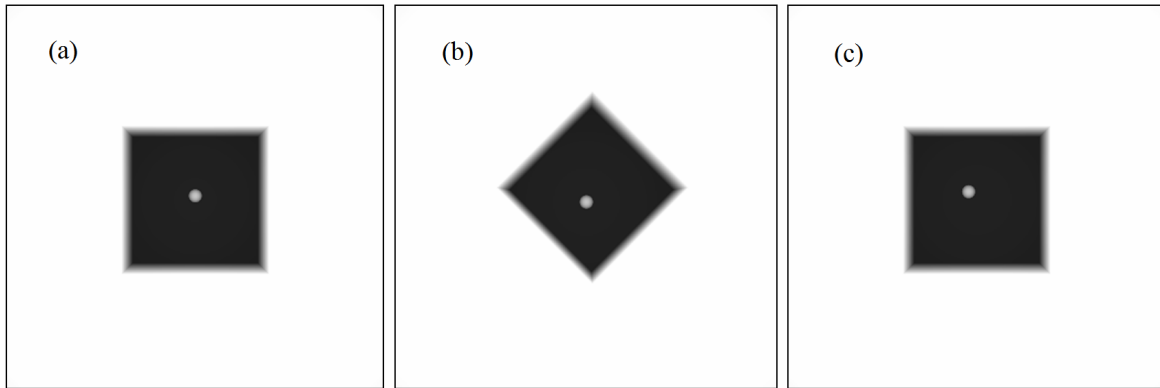


Fig. 12. DTOs generated with a source rotation axe distance equal to 1 meter, an acquisition diameter equal to 1.4 meters, 0.2 meters sensor size, source collimator base distance equal to 0.4 meters, a collimator thickness of 0.08 meters, a field length of 0.05 meters and a ball diameter of 0.005 meters. (a) DTO simulating an image with collimator and table held in  $0^\circ$  and a gantry angle of  $30^\circ$ , a ball misalignment of 0.003 meters with respect to the Y axe is introduced. (b) DTO that simulates an image with gantry and table held in  $0^\circ$  and a collimator angle of  $45^\circ$ , a collimator rotation axe misalignment of 0.003 meters with respect to the X axe is introduces. (c) DTO with gantry and collimator held in  $0^\circ$  and table angle of  $90^\circ$ , a table rotation axe misalignment of 0.003 meters with respect to the X axe is introduced.

### 2.3.3 DICOM conversion

The two-dimensional images are finally converted to DICOM format. A module that creates DICOM file is being used for this purpose<sup>7</sup>. All DICOM fields that are necessary to accomplish the quality control test using our software are added. These fields are the center name, installation name and the patient name.

### 3. RESULTS

A set of DTOs were being generated and controlled using our algorithms. These DTOs are created with a source rotation axis distance equal to 1 meter, an acquisition diameter equal to 1.4 meters, 0.2 meters sensor size, source collimator base distance equal to 0.4 meters, a collimator thickness of 0.08 meter, a field length of 0.05 meter and a ball diameter of 0.005 meter. The control algorithms contain a lot of adjustable parameters as the zoom factor, the interpolation algorithm, the beam detection method (global or local) and the size of the Gaussian kernel.

Results of controlling a set of DTOs with certain amount of rotation axis misalignments are presented below.

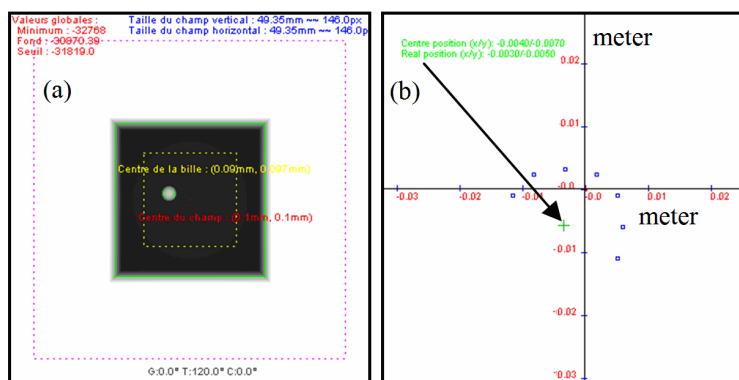


Fig. 13. DTOs generated with a table rotation axis misalignment of 3mm and 5mm with respect to the X (lateral) and Z (longitudinal) axis. Gantry and collimator are held in  $0^\circ$ , while 6 angles are used for the table rotation ( $90^\circ$ ,  $120^\circ$ ,  $150^\circ$ ,  $180^\circ$ ,  $210^\circ$ ,  $240^\circ$  and  $270^\circ$ ). (a) DTO simulating an image with table rotation axis of  $30^\circ$ . (b) Results showing the calculated rotation axis misalignment which retrieves the same input values.

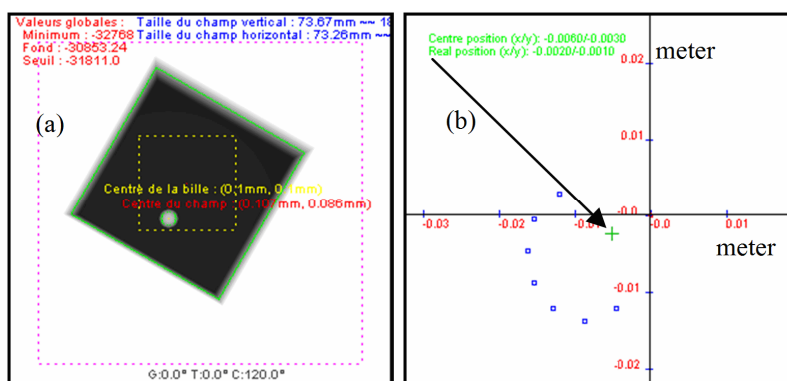


Fig. 14. DTOs generated with a collimator rotation axis misalignment of 2 mm and 1 mm with respect to the X (lateral) and Z (longitudinal) axis. Gantry and collimator are held in  $0^\circ$ , while 6 angles are used for the table rotation ( $90^\circ$ ,  $120^\circ$ ,  $150^\circ$ ,  $180^\circ$ ,  $210^\circ$ ,  $240^\circ$  and  $270^\circ$ ). (a) DTO simulating an image with collimator rotation axis of  $120^\circ$ . (b) Results showing the calculated rotation axis misalignment.

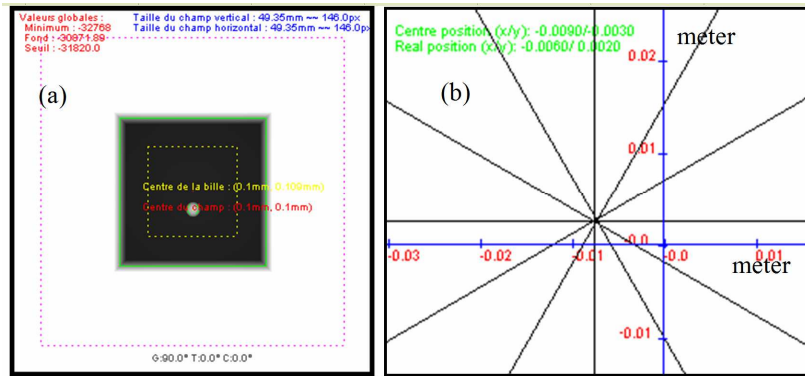


Fig. 15. DTOs generated with a gantry rotation axis misalignment of 6mm and -2mm with respect to the longitudinal and anterior/posterior axis. Table and collimator are held in 0°, while 5 angles are used for the table rotation (0, 30, 60, 90, 120 and 150°). (a) DTO simulating an image with gantry rotation axis of 90°. (b) Results showing the calculated rotation axis misalignment.

Finally, the treatment machine isocentre is calculated using the positions of the gantry, table and collimator rotation centres. In this case the calculated position of treatment machine isocentre is (-0.006, 0.002, -0.0035).

#### 4. DISCUSSION

DTOs were being generated in order to control our algorithms.

A large panel of DTOs with different various calibrated amounts of rotation axis misalignment was being generated. These DTOs are automatically converted to DICOM format and controlled. Results are then compared to the well known amount of rotation axis misalignments initially entered.

Results issued from the application of the QFD-IQC-WL algorithms showed high level of precision. For the misalignment of the tungsten ball with respect to the mechanical isocentre, the level of precision of the calculated position of the centre is equal to the size of the pixel within the zoomed image.

However, this technique shows that errors may occur if: (a) the searching area does not contain the image of the tungsten ball due to a large misalignment of the ball with respect to the mechanical isocentre or if the searching area is too small. (b) The local method for detecting the field is used with images where the gantry and table are held in 0° while the collimator is rotating.

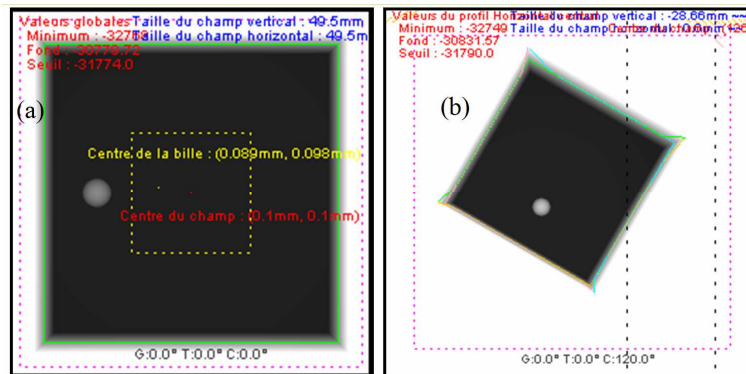


Fig. 16. (a) DTOs generated with ball misalignment of 7mm to the longitudinal axis. The position of the image of the tungsten ball is outside the searching area. (b) Image with gantry and Table held in 0°, while the collimator is rotated to 30°. Errors with detection of the field can be seen in the image.

## 5. CONCLUSION

A technique of generating DTOs which simulate gantry, table and collimator rotation axis misalignments is presented in this paper.

These DTOs confirm that the test proposed by Winston and Lutz is an accurate tool for determining the position and the size of the isocentre, as well as the movements of the sensor. Furthermore, this paper shows that the use of these DTOs is an important method to help verifying all software features.

This technique integrated in the QFD-IQC-WL software allows the user to perform his own auto-tests. This software proves to be an important and easy tool to perform an automated analysis of the test proposed by Winston and Lutz.

The author plans to extend this work by introducing the simulation of the gantry flex map and flat panel movements of linear accelerator into the DTOs.

## REFERENCES

- [1] Lutz W, Winston K R Maleki N. , "A system for stereo tactic radio surgery with a linear accelerator," *Int. J. Radio. Oncol. Biol. Phys.*, 14 373-81 (1988).
- [2] Winkler P., Bergmann H., Stuecklschweiger G., Guss H. , "Introducing a system for automated control of rotation axes, collimator and laser adjustment for a medical linear accelerator," *Physics in Medicine and Biology Volume 48, Number 9*, pp. 1123-1132 (2003).
- [3] J. Pouliot, O. Morin, et al. ,"Megavoltage cone-beam: recent developments and clinical applications," *Cancer radiother*, 10(5): 258-68 (2005).
- [4] Jaffray DA and Siewerdsen JH. , "Cone beam computed tomography with a flat-panel imager: Initial performance characterization," *Med. Phys.*, 27 1311-23 (2000).
- [5] Mackie TR, Kapatoes J, Ruchala K, et al. , "Image guidance for precise conformal radiotherapy," *Int. J. Radiat. Oncol. Biol. Phys.*, 56 89-105 (2003).
- [6] E. Denis, S. Beaumont and JP. Guédon. , "Digital reconstructed radiography quality control with software methods," *SPIE Conf. Medical Imaging - San Diego* (2005).
- [7] E. Denis, JP. Guédon, S. Beaumont and N. Normand. , "Discrete and continuous description of a three dimensional scene for quality control of radiotherapy treatment planning systems," *SPIE Conf. Medical Imaging - San Diego* (2006).
- [8] T. Torfeh, S. Beaumont, JP. Guédon, E. Denis. , "An evaluation of two software tools dedicated for an automatic analysis of the CT scanner image spatial resolution," *IEEE, Engineering in Medicine and Biology Societe. Lyon-France* (August 2007).
- [9] QualiFormeD SARL., <http://www.qualiformed.com>